The Okwa basement complex, western Botswana: U–Pb zircon geochronology and implications for Eburnean processes in southern Africa

R.B.M. Mapeo [a,*], L.V. Ramokate [b], F. Corfu [c], D.W. Davis [d], A.B. Kampunzu [a,✠]

[a] *Department of Geology, University of Botswana, Private Bag UB00704, Gaborone, Botswana*
[b] *Botswana Geological Survey, Private Bag 14, Lobatse, Botswana*
[c] *University of Oslo, Geological Museum, P.B. 1172 Blindern, N-0318 Oslo, Norway*
[d] *Department of Geology, University of Toronto, 22 Russell Street, Toronto, Ont., Canada M5S 3B1*

Received 15 September 2005; received in revised form 27 May 2006; accepted 30 May 2006
Available online 24 July 2006

Abstract

The Okwa Basement Complex crops out at the northwestern edge of the Kaapvaal craton within the Okwa Inlier, an isolated exposure of Precambrian basement in the Kalahari Desert. New U–Pb zircon dating was performed on all the major Palaeoproterozoic lithologies of the complex. Results are 2055.3 ± 1.3 Ma for augen gneiss, 2056.3 ± 1.3 Ma for foliated monzogranite and 2057 ± 2 Ma for microgranite. A meta-rhyolite gives an age of 2055 ± 4 Ma, based on one concordant zircon, and contains an inherited zircon with an age of 2101 ± 4 Ma. All precisely dated rocks are indistinguishable in age at 2056 ± 2 Ma. This age can be broadly correlated with Palaeoproterozoic geologic events in the Magondi belt at the northwest margin of the Zimbabwe craton and the Triangle Shear Zone in the Limpopo belt. However, the most precise correlation is with the Bushveld Complex, whose age is indistinguishable from that of the Okwa Basement Complex. This suggests a link between marginal and intra-cratonic Bushveld-age magmatism on the Kaapvaal craton.

Keywords: Palaeoproterozoic; U–Pb zircon ages; Eburnean; Bushveld magmatism; Okwa; Botswana; Africa

1. Introduction

Major Proterozoic belts bound the northwestern margin of the Archaean Kaapvaal-Limpopo-Zimbabwe craton in Botswana. They are largely concealed beneath a cover of Phanerozoic sediments (Karoo Supergroup and Kalahari Group) but their continuity can be inferred by combining geophysical information, borehole data and available outcrops (Fig. 1). Correlation of Proterozoic units in Botswana with orogenic systems in neighbouring countries is generally hampered by the paucity of modern geochronological work that relates isotopic ages to tectono-magmatic events. In this paper we report new precise U–Pb dates of zircons from the Okwa Basement Complex in western Botswana and discuss the regional implications of these data for the Palaeoproterozoic Eburnean crustal evolution of southern Africa.

2. Geological setting

The Palaeoproterozoic Okwa Inlier (Fig. 2) is situated in western Botswana. It is bounded by the Archaean Kaapvaal craton (Moore et al., 1993; Kamo et al., 1995) to the southeast and is unconformably overlain by sedimentary rocks of the Neoproterozoic Ghanzi-Chobe belt to the northwest (Fig. 3; Schwartz et al., 1996; Modie, 1996).

* Corresponding author. Tel.: +267 355 2536; fax: +267 318 5097.
E-mail addresses: mapeorbm@mopipi.ub.bw (R.B.M. Mapeo), Lvramokate@gov.bw (L.V. Ramokate), fernando.corfu@nhm.uio.no (F. Corfu), dond@geology.utoronto.ca (D.W. Davis), Kampunzu@mopipi.ub.bw (A.B. Kampunzu).
✠ Deceased, 2004.

1464-343X/$ - see front matter © 2006 Elsevier Ltd. All rights reserved.
doi:10.1016/j.jafrearsci.2006.05.005

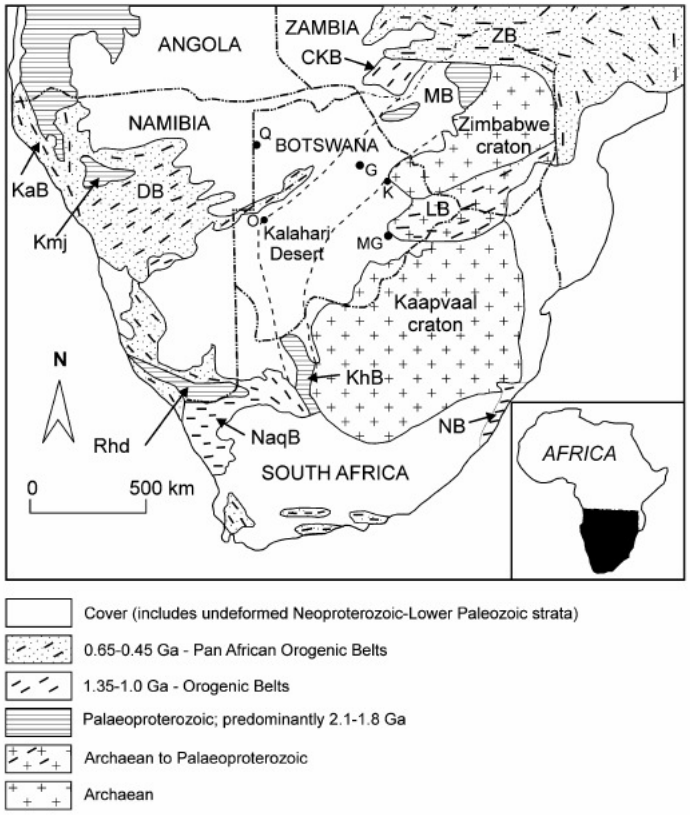

Fig. 1. The tectonic framework of southern Africa showing the main Archaean terrains and inferred subsurface extents of Proterozoic belts. O: Okwa Inlier; Q: Quangwadum valley; K: Kubu Island; G: Gweta Complex; KhB: Kheis Belt; NaqB: Namaqua belt; KaB: Kaoko belt; DB: Damara Belt; CKB: Choma-Kalomo block; ZB: Zambezi belt; MB: Magondi belt; MG: Mahalapye Granite; LB: Limpopo belt; NB: Natal belt; Kmj: Kamanjab Inlier; Rhd: Richtersveld province (modified from Singletary et al., 2003; Rainaud et al., 2005).

The exposures in the Okwa valley have been described by Crockett and Jennings (1965), Bossum and Lüdtke (1980), Key and Rundle (1981), Aldiss (1988), Aldiss and Carney (1992) and Ramokate (1998). The Okwa Basement Complex experienced several episodes of folding, thrusting and brittle faulting, which are thought to range from Mesoproterozoic (Kibaran) to Karoo in age.

The first attempt to date the rocks in the Okwa valley established its Palaeoproterozoic age and enabled a correlation with the Kheis Belt 200 km to the South (Mallick et al., 1981) and with other Eburnean crustal provinces in southern Africa (Key and Rundle, 1981; Stowe et al., 1984; Hartnady et al., 1985). Despite this broad scale correlation, the protolith age of the Okwa Basement Complex is highly debated. Whole-rock Rb–Sr errorchrons of gneissic rocks and microgranite yielded ages of 1813 ± 68 Ma ($^{87}Sr/^{86}Sr_i = 0.7227$, MSWD = 24) and 1004 ± 49 Ma ($^{87}Sr/^{86}Sr_i = 0.7217$, MSWD = 7.5), respectively (Key and Rundle, 1981). K–Ar isotope determinations on separated biotites indicated ages between 1156 ± 28 Ma and 1093 ± 36 Ma, while two samples of hornblende from enclaves in augen gneiss gave K–Ar dates of 1971 ± 31 Ma and 1193 ± 35 Ma. All authors agree that the Mesoproterozoic Rb–Sr and K–Ar dates mark an isotopic resetting of both isotopic systems during a younger event. Key and Rundle (1981) suggested that the igneous protolith of the Okwa Basement Complex is about 1831 Ma old, whereas Aldiss and Carney (1992) consider that this is the age of a local Palaeoproterozoic tectonometamorphic event. The older date of 1971 ± 31 Ma quoted above was interpreted to be the age of the protolith of this basement. The enclaves in the Okwa augen gneiss were reported to be xenoliths (Key and Rundle, 1981) or dykes (Aldiss and Carney, 1992). New investigations indicate that the augen gneiss contains both micaceous restites and mafic microgranular enclaves. The mafic enclaves are

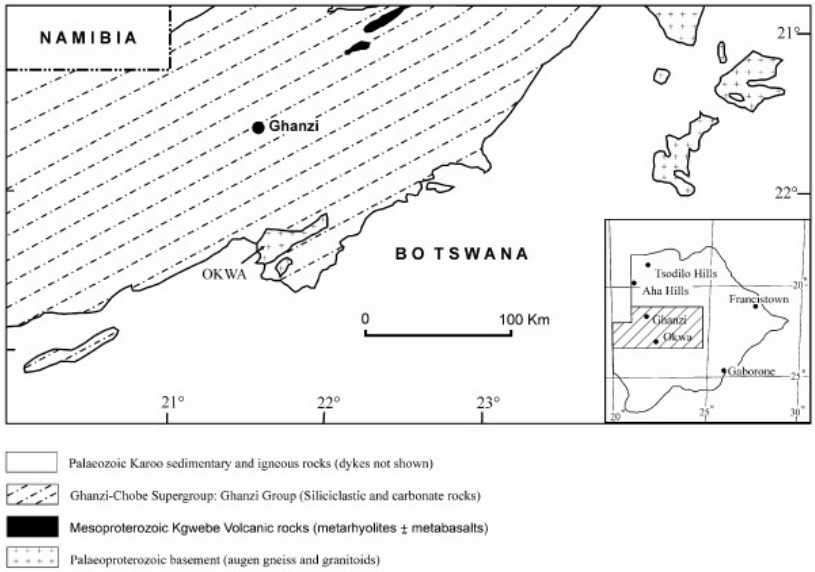

Fig. 2. Geological map of northwestern Botswana showing the location of the Okwa Basement Complex and various other important geological formations. Inset: Position of the main map in Botswana.

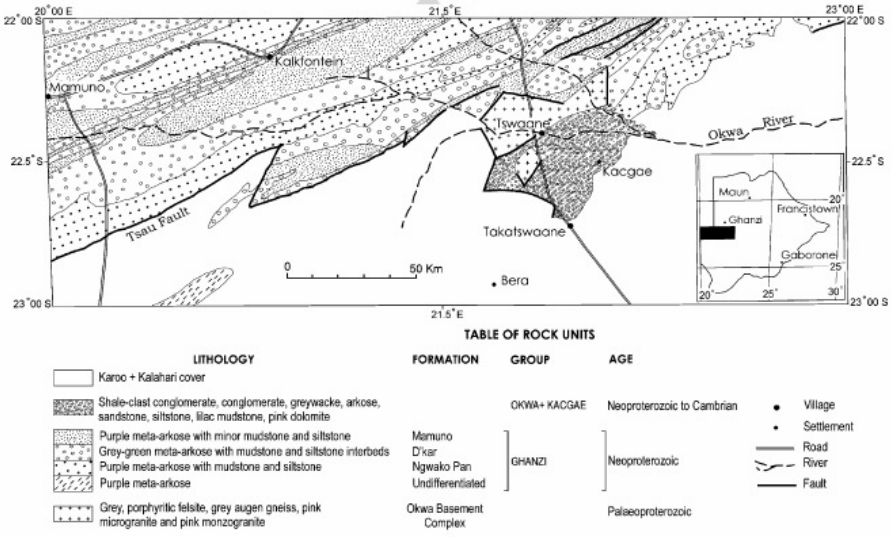

Fig. 3. Geological map of Ghanzi-Makunda area showing the location of the Okwa Basement Complex (Ramokate et al., 2000). This map combines both the surface and subcrop extent of the Okwa Basement Complex. Inset: Position of the main map in Botswana.

interpreted to represent mixing between mafic and felsic magmas (e.g., Didier and Barbarin, 1991).

The Okwa Basement Complex (Fig. 4) consists of four main lithologies:

(1) Feldspar-phyric meta-rhyolite represents the oldest unit in the area (Aldiss and Carney, 1992; Ramokate, 1998). It is intruded by granitoid veins, and xenoliths of the meta-rhyolite occur within the granite. The

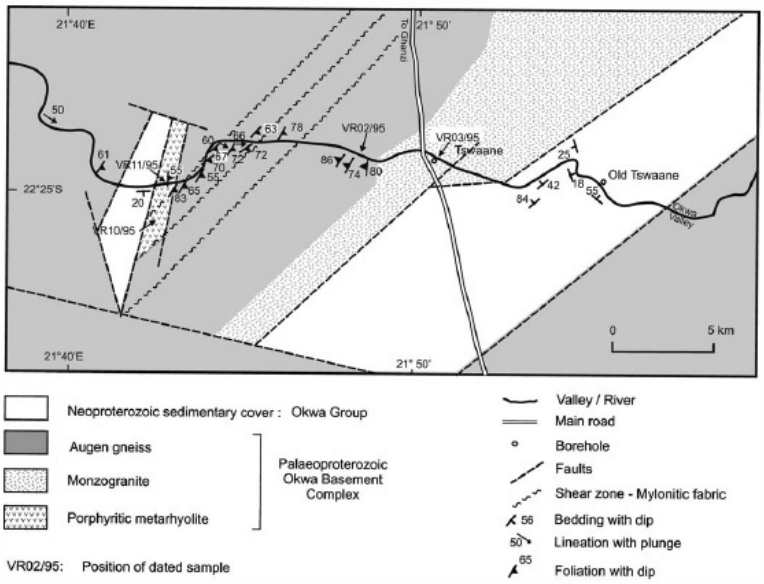

Fig. 4. Geological map showing then subcrop and outcrop main lithologies of the Okwa Basement Complex in outcrop and subcrop and locations of the samples dated by U–Pb zircon technique.

meta-rhyolite contains a main NNE–SSW tectonic fabric, which dips moderately to steeply to the SSE (55–83°). The rock is grey, aphyric to fine-grained, homogeneous, and highly foliated with sparse, euhedral quartz and pink sodic plagioclase phenocrysts and flattened biotite clumps (fiamme?). The phenocrysts are about 2 mm across and are set in a fine-grained granoblastic matrix of quartz, feldspar, muscovite, biotite, sphene and opaque minerals.

(2) Pink-grey to pink mylonitic augen gneiss (monzogranite in composition) locally contains feldspar megacrysts and is marked by a NE–SW-trending foliation (S_1) wrapping oriented pink and white feldspar augen. These megacrysts are commonly rimmed by white plagioclase feldspar, forming a rapakivi texture. The megacrysts are commonly euhedral (oval ones are also present), in spite of the intense deformation. Mafic microgranular and micaceous enclaves are flattened within the S_1 plane. The S_1 foliation cuts directly across the contact between enclaves and the host rocks. Petrographically, the augen gneiss is composed of quartz, microcline, oligoclase, biotite, hornblende, sphene, and opaque minerals. The plagioclase is sericitised, while the hornblende is chloritised, indicating a retrograde metamorphism. A penetrative, gneissic fabric is present throughout the rock with a strong, down-dip, mineral-elongation lineation. The gneissic fabric is defined by the alignment of biotite and other mafic minerals, and by recrystallisation of quartz into elongate ribbons. The K-feldspar megacrysts are highly resistant to deformation and define the augen texture.

(3) Weakly foliated, pink to purple, K-feldspar-rich monzogranite contains a foliation concentrated within spaced shear bands that are parallel to S_1 in the augen gneiss. No grain size change occurs in the monzogranite when approaching the augen gneiss. The transition from augen gneiss to the pink monzogranite is not exposed but is interpreted to be gradational, suggesting synchronous emplacement of their granitic protoliths. In thin section the K-feldspar rich monzogranite consists of quartz, microcline, microperthite, oligoclase, biotite, sericite, sphene and haematite. The oligoclase is commonly sericitised, while the biotite is partly replaced by chlorite or sericite. A penetrative gneissic foliation locally occurs in the monzogranite, but it is not as intense as in the augen gneisses and generally tends to intensify into narrow shear zones trending SW–NE. The foliation is caused by the alignment of biotite and sericitic muscovite.

(4) An aplitic microgranite typically contains a weak, homogeneous S_1 foliation defined primarily by oriented biotite flakes and white microporphyritic feldspars. The microgranite forms veins intruding the meta-rhyolite, granitic augen gneiss and monzogranite and is the youngest granitic facies. The exposed veins are between 10 m and 50 m in thickness. There are no granitic veins intruding the microgranite

although it is cut by post-tectonic quartz veins. The microgranite is pink or grey, medium grained, leucocratic, homogeneous and foliated. Petrographically, it is composed of quartz, microcline, oligoclase, biotite, sphene, zircon and opaque minerals. The same penetrative gneissic fabric found in the granitic augen gneiss can be found locally in the microgranites.

The latter three lithologies form part of a granite complex now deformed into augen gneiss over most of the area, especially along ductile shear zones shown in Fig. 4. In some areas the augen gneiss contains enclaves of microgranite. These enclaves have sinuous, invaginated contacts with the gneiss and no sharp contacts have been observed between the two rock types. Dykes of the same microgranite show gradational contacts against the gneiss. The penetrative S_1 foliation can be traced directly across the augen gneiss into the microgranite but is developed much more weakly in the latter. These features imply that the two rock types represent penecontemporaneous magmas but were emplaced over some length of time during the deformation, with the younger microgranite recording less strain. The microgranite intrudes the meta-rhyolite, which is cut by a network of microgranitic and quartz veins. These veins are parallel to S_1 in the meta-rhyolite, and in the augen gneiss and microgranite. Therefore, the granitoid rocks in the Okwa Basement Complex appear to be synkinematic with respect to S_1. This interpretation is similar to that of Haslam (1978) quoted in Key and Rundle (1981). Preserved euhedral quartz and feldspar phenocrysts in a microgranular groundmass indicate a volcanic or subvolcanic origin for the meta-rhyolite.

U–Pb isotopic data were obtained on twelve zircon fractions extracted from four samples of the Okwa Basement Complex (Fig. 4). These samples are representative of the four main lithologies present, viz. feldspar phyric meta-rhyolite (sample VR 11/95), augen gneiss (sample VR 02/95), foliated monzogranite (sample VR 03/95) and microgranite (sample VR 10/95).

3. Analytical procedure

The four samples, weighing between 2 and 3 kg each, were dated at the Jack Satterly Geochronology Laboratory in the Royal Ontario Museum, Toronto. Crushing and mineral separation followed standard procedures. Minerals were hand picked under a binocular microscope to avoid visible imperfections. All zircon fractions selected for analysis were subjected to air abrasion (Krogh, 1982). Before digestion all zircons fractions were washed in 4 N HNO_3. Zircon was dissolved in HF in Teflon bombs at 200 °C. Pb and U were separated from Zr using anion-exchange columns in HCl media. Total procedure blanks are normally 1–3 pg Pb and 0.1 U for the HCl in the microcolumn technique applied to zircon. Occasional higher excursions may be due to dust particles. All initial common Pb was corrected assuming the isotopic composition of laboratory blank. Pb and U were loaded on Re filaments with silica gel and analysed with a VG-354 mass spectrometer in a single collector mode. Uncertainties of individual analyses are reported at 2 sigma and were propagated using an in-house program that accounts for most sources of errors in the U–Pb analyses. Discordia lines and weighted average calculations were done using the program of Davis (1982). Errors are quoted at the 95% confidence level.

4. Results

The analytical results are summarised in Table 1.

4.1. Grey, feldspar-phyric meta-rhyolite (sample VR 11/95)

The sample yielded a relatively small amount of zircons. Most of them are euhedral, short, prismatic crystals showing prominent development of {1 0 0} and {1 0 1} crystal faces; they generally also contain abundant inclusions and rusty cracks.

Three analyses were done (1–3, Table 1, Fig. 5a). One fraction obtained from pieces of cracked euhedral crystals resulted in analysis 3, which is 15% discordant. This result was considerably improved by analysis of one euhedral crystal (analysis 2) that is concordant at 2055 ± 4 Ma. A third analysis on a clear zircon fragment (analysis 1) is also concordant but has an age of 2101 ± 4 Ma. This zircon is interpreted as a xenocrystic. Apparent cores are visible in some crystals from this sample, and it was inferred that most of the better-looking grains, including the one which yielded analysis 2, may have xenocryst cores. By contrast the grains used for analysis 3 were chosen specifically among those zircons least likely to have inheritance. The $^{207}Pb/^{206}Pb$ age of 2041 Ma for the latter represents at a minimum age for the pure magmatic component, and supports the validity of the 2055 Ma age defined by analysis 2.

4.2. Grey augen gneiss (sample VR 02/95)

Zircons in this rock are generally uncracked and fairly fresh. Grains are medium to small, euhedral, elongate to stubby prisms with well-developed low-order crystal faces on sides and tips. Many grains contain abundant small, round, colourless inclusions. The colour varies from colourless to pale brown. Colourless cores were seen in a few grains.

Three fractions were analysed, two of which consisted of single relatively large grains chosen to represent the colourless and brownish zircons. A third, multigrain fraction consisted of a mixed population of colourless and brownish zircons. All three abraded fractions gave concordant or near-concordant analyses with similar $^{207}Pb/^{206}Pb$ ages (analyses 4–6, Table 1, Fig. 5b). Fitting these data to a line forced through zero gives an upper Concordia intercept age of 2055.3 ± 1.3 Ma with a 78% probability of fit, which is well within acceptable limits for mutual agreement of the data points.

Table 1
ID-TIMS U–Pb data for zircon from the Okwa Granitoids

No.	Zircon fraction characteristics (a)	Weight (μg) (b)	U (ppm)	Th/U (c)	Pbc (pg) (d)	$^{206}Pb/^{204}Pb$ (measured) (e)	$^{206}Pb/^{238}U$ (f)	± (g)	$^{207}Pb/^{235}U$ (f)	± (g)	$^{207}Pb/^{206}Pb$ (Ma) (f)	± (g)	Disc. (%)
Sample VR 11/95 meta-rhyolite													
1	1 Fragment	1	140	0.55	2.5	1378	0.3832	18	6.880	39	2100.9	4.1	0.5
2	1 Euhedral	1	85	0.49	1.0	1939	0.3749	19	6.558	39	2054.8	4.1	0.1
3	5 Euhedral	1	200	0.47	2.3	1755	0.3180	15	5.517	31	2040.9	3.8	14.6
Sample VR 02/95 augen gneiss													
4	1 Clear	2	190	0.59	1.0	8714	0.3762	12	6.580	22	2055.1	1.8	−0.2
5	1 Brown	3	90	0.44	3.1	2084	0.3753	18	6.571	30	2056.9	4.8	0.2
6	30 Clear, Brown	26	260	0.50	8.4	19196	0.3735	14	6.534	26	2055.3	2.6	0.5
Sample VR 03/95 foliated monzogranite													
7	1 Clear	5	70	0.48	0.8	10414	0.3767	14	6.596	22	2057.1	4.0	−0.2
8	1 Brown	5	220	0.31	1.5	16757	0.3754	12	6.570	22	2056.1	2.4	0.1
9	25 Brown, Euhedral	35	270	0.39	2.6	84856	0.3757	12	6.560	22	2056.4	2.0	0.3
Sample VR 10/95 microgranite													
10	13 Euhedal	1	310	0.60	0.8	9057	0.3733	17	6.536	34	2056.5	2.7	0.6
11	Euhedral tips and fragments	4	260	0.54	2.8	8731	0.3703	18	6.471	36	2053.2	2.7	1.3
12	Euhedral tips and fragments	3	270	0.50	2.1	8769	0.3689	18	6.448	35	2053.8	2.7	1.7

(a) Descriptions and number of zircon grains analysed; (b) uncertainties less than 10% for weights of more than 10 μg, and about 50% for weights of about 1 μg. The uncertainty in the weight directly applies to the corresponding U concentration; (c) Th/U model value calculated from $^{208}Pb/^{206}Pb$ ratio and age of sample; (d) Pbc: total common Pb in analyses, includes blank and initial common Pb; (e) measured ratio corrected for spike and fractionation; (f) corrected for spike, fractionation, blank and initial common Pb; (g) errors are absolute values and represent 2 sigma.

4.3. Purple foliated monzogranite (sample VR 03/95)

The zircon population from this rock consists of medium to large grains. Most are cracked and altered but the smaller grains are relatively fresh. As with the previous sample, the zircons are euhedral, elongate to stubby prisms with well-developed low-order crystal faces and bubble-like inclusions, and they vary from colourless to pale brown. The tips of the zircons tend to be asymmetrical, unlike those from sample VR 02/95.

Two single zircons of different colour plus a multigrain, mixed fraction were analysed and gave data points with indistinguishable $^{207}Pb/^{206}Pb$ ages (analyses 7–9, Table 1, Fig. 5c). Regressing these data to a line forced through zero gives an upper intercept age of 2056.3 ± 1.3 Ma with a 90% probability of fit.

4.4. Pink microgranite (sample VR 10/95)

The zircon population in this rock is qualitatively similar to that of sample VR 11/95, but the zircon is more abundant, permitting a wider selection of the most suitable grains. Analyses were carried out on three multigrain fractions of highly abraded crystals and fragments thereof (analyses 10–12, Table 1, Fig. 5d). They yield three somewhat discordant data points with comparable $^{207}Pb/^{206}Pb$ ages of 2057–2053 Ma. The lack of spread prevents the calculation of a discordia line from the three analyses alone, but projections through lower intercepts between 0 and 500 Ma yield a range of possible upper intercept ages between 2055 and 2058 Ma, from which a best estimate of 2057 ± 2 Ma is derived.

4.5. Discussion

The U–Pb zircon ages for all the dated rocks are identical within analytical uncertainties. The ages and errors of the precisely dated plutonic rocks (augen gneiss, foliated monzogranite and microgranite) are encompassed within the time range 2056 ± 3 Ma. This gives strong support to our field interpretation that all these lithologies are part of a single major igneous event, with progressive transition between the intrusive bodies (no chilled margins or discordant igneous foliations). Field evidence indicates that the microgranite intrudes the feldspar-phyric meta-rhyolite but their close similarity in age indicates that the meta-rhyolite represents part of the same magmatic event as the Okwa plutonic rocks. The oldest age of 2101 ± 4 Ma is interpreted to date a xenocryst. A similar inherited component in the meta-rhyolite may be present in other zircon grains from that sample that contains visible cores. The 2101 Ma age provides evidence for the existence of relatively young Palaeoproterozoic crustal components in the study area at the time the exposed units of the Okwa Basement Complex were emplaced approximately 50 Ma later.

Earlier attempts to document the age of the Okwa Basement Complex in western Botswana using Rb–Sr and K–Ar techniques gave ages younger than 2 Ga. These ages can now be confidently taken as marking episodes of partial or complete resetting of these isotopic systems dur-

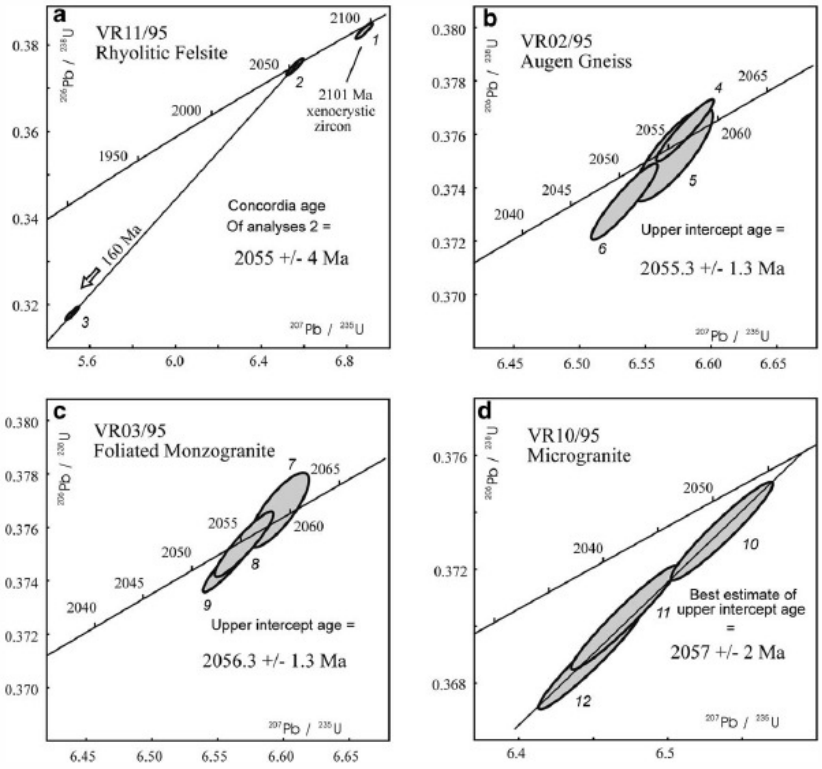

Fig. 5. (a)–(d) Concordia diagrams of zircon fractions from the Okwa Basement Complex.

ing younger tectono-metamorphic events. The new U–Pb zircon dating confirms the Palaeoproterozoic age of the Okwa Basement Complex and indicates it is similar in age to the Richtersveld province (which has Sm–Nd ages between 2089 and 1996 Ma, and U–Pb zircon crystallisation ages of between 1792 ± 18 Ma and 1747 ± 11 Ma) West of the Kaapvaal craton in the Namaqua province (Becker et al., 1996; Reid, 1997). Comparison is drawn with the Quangwadum Complex augen gneisses and granites (with a $^{207}Pb/^{206}Pb$ zircon crystallisation age of 2050.5 ± 0.6 Ma) north of the Okwa Complex, near the Botswana–Namibia border in the West (Singletary et al., 2003), and with the Kheis-Magondi belt along the northwestern edges of the Kaapvaal-Zimbabwe cratons (Stowe, 1986; Munyanyiwa et al., 1995; Cornell et al., 1998; Mapeo et al., 2001; McCourt et al., 2001). The trend of the Magondi belt towards the southwest is buried, but geophysical data suggests the possibility of a connection with the Kheis belt on the northwestern margin of the Kaapvaal craton (Reeves, 1978) (Fig. 1). Magondi belt rocks intersected in a borehole at Gweta in NE Botswana comprise high-grade paragneisses (Carney and Dowsett, 1991; Carney et al., 1994). The Magondi Supergroup meta-sedimentary rocks were deposited after ≈2.125 Ga metamorphosed and deformed between 2027 ± 8 and 1997 ± 2.6 based on SHRIMP U–Pb zircon dating of paragneisses and late to synkinematic granites (Mapeo et al., 2001; McCourt et al., 2001). South of Gweta borehole, granitoids rocks exposed at Kubu Island yielded U–Pb zircon ages of 2039 ± 1 (Majaule et al., 2001), indicating a southward extension of granitoids rock emplaced during orogenesis in the Magondi belt. Farther south of these small outcrops at Kubu Island the Mahalapye Granite at the western extremity of the central Limpopo belt yielded a SHRIMP U–Pb zircon crystallisation age of 2023 ± 7 Ma (McCourt and Armstrong, 1998).

Rainaud et al. (2005) describe ≈2050–1850 Ma magmatic arc terrane that extends from south-western Zambia and the Democratic Republic of Congo into northern Namibia and NW Botswana, defining a Palaeoproterozoic magmatic arc termed the Kamanjab-Bangweulu terrane. Key units in Zambia are rocks of the 'Lufubu Metamorphic Complex' formed between 2050 and 1850 Ma, and in northern Namibia granitic gneiss of the Tsumkwe inlier yielded a SHRIMP U–Pb zircon age of 2022 ± 15 Ma (Hoal et al., 2000). The Tsumkwe gneisses are similar to the Quangw-

adum Complex augen gneisses and granites to the North along the Botswana–Namibia border, North of the Okwa Basement Complex (Singletary et al., 2003; Rainaud et al., 2005). However, all of the Palaeoproterozoic rocks described above are separated from the Okwa Basement Complex by an inferred subsurface extension of the Pan-African Damara belt (Hanson, 2003; Singletary et al., 2003), and possible relations between Palaeoproterozoic units on either side of this younger orogen remain unclear.

An ≈2-Ga tectono-metamorphic event has also been documented in the Triangle Shear Zone of the Limpopo Belt (Kamber et al., 1995) and is inferred to mark a major Palaeoproterozoic dextral shear zone (McCourt and Vearncombe, 1992; Rollinson and Blenkinsop, 1995). Barton et al. (2003) have shown that this tectono-metamorphic event in the Limpopo belt may have been accompanied by the emplacement of tonalities, granodiorites and granites at ≈2.0–1.9 Ga. The Okwa Basement Complex and the Kheis-Magondi belt may represent a partly buried geographically continuous although diachronous Palaeoproterozoic orogenic system in the Kalahari craton active at the same time as the emplacement of the Bushveld Igneous Complex (Hanson, 2003; Rainaud et al., 2005).

The best constrained temporal correlation is with emplacement of the Bushveld Complex, which now has a precise age determination of between 2060 ± 2 and 2055 ± 2 Ma (Walraven and Hattingh, 1993; Walraven, 1997; Buick et al., 2001; Eglington and Armstrong, 2004; Mapeo et al., 2004). The Lebowa Granite Suite (comprising Nebo, Makhutso and Steelport Park granites) of the Bushveld Complex was emplaced between 2058 ± 4 and 2053 ± 4 Ma, which is indistinguishable from the ages at Okwa (Harmer and Armstrong, 2000). The Okwa age is also similar to ages of the Critical Zone of the Rustenburg Layered Suite which yielded SHRIMP and IDTIMS zircon ages of 2054 ± 3 Ma and 2056 ± 2 Ma, respectively (Harmer and Armstrong, 2000). This suggests a link between magmatism at the margin of the Kaapvaal craton and major intra-cratonic magmatism. Intrusion of the Bushveld mafic-ultramafic rocks is associated with coeval emplacement of a large volume of felsic magmas (Walraven, 1985; Hatton and Schweitzer, 1995; Schweitzer et al., 1995), and Bushveld-type intrusive complexes occur in SE Botswana (e.g., Moshaneng and Kukong areas), where recently obtained $^{207}Pb/^{206}Pb$ zircon emplacement ages range between 2060 ± 3 and 2053 ± 4 Ma (Lock et al., 2002; Mapeo et al., 2004). Although Bushveld magmatism is exposed 500 km away from Okwa near the middle of the Kaapvaal craton, it represents the largest single igneous body ever documented, and is on the order of hundreds of kilometers across. Its generation would have required an unusually extensive degree of mantle melting. The close age correspondence between the Bushveld intrusion and Okwa rocks suggests that crustal melting associated with the thermal anomaly that produced the Bushveld magmas may have been much more extensive than previously thought.

5. Conclusions

New U–Pb zircon data indicate that igneous rocks of the Okwa Basement Complex in western Botswana were emplaced over a narrow time span of 2056 ± 3 Ma. This age places the Okwa rocks within the Eburnean–Ubendian orogenic system in Africa. The age of the Okwa Basement Complex is indistinguishable from precise ages reported for the Bushveld complex in South Africa suggesting a link between marginal and intra-cratonic Bushveld-age magmatism at this time.

Acknowledgements

LVR benefited from the use in the field of aerial photographs of the Okwa Valley annotated by Don Aldiss and Gerhard Lüdtke during the geological survey in winter of 1994. We also greatly benefited from the fruitful discussions in the field with Roger Key, Richard Hanson and other geologists of the Regional Geology Division of the Geological Survey. We are grateful to the Botswana Government for financing the geochronological work and to Roger Key for his comments on a first draft of this paper. A.B.K. and R.B.M.M. acknowledge the support from the University of Botswana/FoS-RPC (Project #R442) for Research in Central and NW Botswana. The paper benefited from reviews by the Journal of African Earth Sciences reviewers. Initial reviews were also carried out by M. de Wit and J.D. Kramers. The diagrams were drafted by Mr. O.T. Okatswa. This paper is published with the authorisation of the Minister of Mineral Resources and Water Affairs, and of the Director of the Geological Survey Department, Botswana.

References

Aldiss, D.T., 1988. The pre-Cainozoic geology of the Okwa Valley near Tswaane borehole. Botswana Geological Survey, Lobatse, Botswana Bulletin 34, 50p.

Aldiss, D.T., Carney, J.N., 1992. The geology and regional correlation of the Proterozoic Okwa Inlier, western Botswana. Precambrian Research 56, 255–274.

Barton, J.M., Barnett, W.P., Barton, E.S., Barnett, M., Doorgapershad, A., Twiggs, C., Klemid, R., Martin, J., Mellonig, L., Zengelein, R., 2003. The geology of the area surrounding the Venetia Kimberlite pipes, Limpopo belt, South Africa: a complex interplay of nappe tectonics and granitoid magmatism. South African Journal of Geology 106, 109–128.

Becker, T., Hansen, B., Weber, K., Wiegand, B., 1996. U–Pb and Rb–Sr isotopic data for the Mooirivier Complex, Weener Igneous Suite and Gaub valley Formation (Rehoboth Sequence) in the Nauchas area and their significance for Palaeoproterozoic crustal evolution in Namibia. Namibia Geological Survey Communications 11, 31–46.

Bossum, W., Lüdtke, G., 1980. Ground geophysical, geochemical and geological investigations in selected areas of the Kalahari. Final Report of Phase 1 (1979) of the GS17 BGR project (the German contribution to the Exploration of the Kalahari). Geological Survey of Botswana, unpublished, p. 319.

Buick, I.S., Maars, R., Gibson, R., 2001. Precise U–Pb titanite age constraints on the emplacement of the Bushveld Complex, South Africa. Geological Society of London 158, 3–6 (special publication).

Carney, J., Aldiss, D.T., Lock, N.P., 1994. Geology of Botswana. Geological Survey, Ministry of Mineral Resources and Water Affairs, Lobatse, Botswana, Bulletin 37, 113pp.

Carney, J.N., Dowsett, J.S., 1991. Lithological information from a borehole cored through cover and basement rocks near Gweta and its bearing on the distribution of major crustal boundaries in Botswana. Botswana Journal of Earth Sciences 1, 1–13.

Cornell, D.H., Armstrong, R.A., Walraven, F., 1998. Geochronology of the Proterozoic Hartley Baslat Formation, South Africa: constraints on the Kheis tectonogenesis and the Kaapvaal craton's earliest Wilson Cycle. Journal of African Earth Sciences 26, 5–27.

Crockett, R.N., Jennings, C.M.H., 1965. Geology of part of the Okwa Valley, western Bechuanaland. Records of the Geological Survey of Botswana (1961–62), 101–113.

Davis, D.W., 1982. Optimum linear regression and error estimation applied to U–Pb data. Canadian Journal of Earth Sciences 19, 2141–2149.

Didier, J., Barbarin, B. (Eds.), 1991. Enclaves and Granite Petrology. Developments in Petrology, vol. 13. Elsevier, Amsterdam, p. 625.

Eglington, B.M., Armstrong, R.A., 2004. Kaapvaal craton and adjacent orogens, southern Africa: a geochronological database and overview of the geological development of the craton. South African Journal of Geology 107, 13–32.

Hanson, R.E., 2003. Proterozoic geochronology and tectonic evolution of southern Africa. In: Yoshida, M., Windly, B.F., Dasgupta, S. (Eds.), Proterozoic East Gondwana: Supercontinent Assembly and Break. Geological Society of London 206, 427–463 (special publication).

Harmer, R.E., Armstrong, R.A., 2000. Duration of the Bushveld Complex (seno lato) magmatism: constraints from new SHRIMP zircon chronology. Abstaracts and program, Workshop on the Bushveld Complex, Gethane Lodge, Burgersfort, South Africa.

Hartnady, C.J.H., Joubert, P., Stowe, C., 1985. Proterozoic crustal evolution in southwestern Africa. Episodes 8, 236–244.

Haslam, H.W., 1978. Interim Report, dated 9 November 1978. Mineral Unit, Institute of Geological Sciences, London, unpublished.

Hatton, C.J., Schweitzer, J.K., 1995. Evidence for synchronous extrusive and intrusive Bushveld magmatism. Journal of African Earth Sciences 21, 259–594.

Hoal, K.O., Hoal, B.G., Griffin, W.L., Armstrong, R.A., 2000. Characterisation of the age and nature of the lithosphere in the Tsumkwe region, Namibia. In: Miller, R.McG. (Ed.), Henno Martin Commemorative Volume. Communications of the Geological Survey of Namibia 12, 21–28 (special issue).

Kamber, B.S., Kramers, J.D., Napier, R., Cliff, R.A., Rollinson, H.R., 1995. The Triangle Shear Zone, Zimbabwe, revisited: new data document an important event at 2.0 Ga in the Limpopo Belt. Precambrian Research 70, 191–213.

Kamo, S.L., Key, R.M., Daniels, L.R.M., 1995. New evidence for Neoarchaean, hydrothermally altered granites in south central Botswana. Journal of the Geological Society of London 152, 747–750.

Key, R.M., Rundle, C.C., 1981. The regional significance of new isotopic ages from Precambrian windows through the Kalahari Beds in northwestern Botswana. Transactions of the Geological Society of South Africa 84, 51–66.

Krogh, T.E., 1982. Improved accuracy of U–Pb zircon ages by the creation of more concordant systems using an air abrasion technique. Geochimica Cosmochimica Acta 46, 637–649.

Lock, N.P., Robb, L.J., Mapeo, R.B.M., Armstrong, R.A., Poujol, M., Respaut, J.P., 2002. Kukong volcanics and metasediments south central Botswana – the felsic accumulation of the Molopo Farms Complex. In: 11 Quadrennial IAGOD Symposium and Geo-congress 2002. Geological Survey of Namibia (Abstract volume in CD format).

Majaule, T., Hanson, R.E., Key, R.M., Singletary, S.J., Martin, M.W., Bowring, S.A., 2001. The Magondi belt in northeast Botswana: regional relations and new geochronological data from Sua Pan area. Journal of African Earth Sciences 32, 257–267.

Mallick, D.I.J., Habgood, F., Skinner, A.C., 1981. A geological interpretation of Landsat imagery and photography of Botswana. Institute of Geological Sciences Overseas Geology and Mineral Resources Report number 56, pp. 1–35.

Mapeo, R.B.M., Armstrong, R.A., Kampunzu, A.B., 2001. SHRIMP U–Pb zircon geochronology of gneisses from the Gweta borehole, NE Botswana: implications for the Palaeoproterozoic Magondi Belt in southern Africa. Geological Magazine 138, 299–308.

Mapeo, R.B.M., Kampunzu, A.B., Ramokate, L.V., Corfu, F., Key, R.M., 2004. Bushveld-age magmatism in southeastern Botswana: evidence from U–Pb and Titanite geochronology of the Moshaneng complex. South African Journal of Geology 107, 219–232.

McCourt, S., Armstrong, R.A., 1998. SHRIMP U–Pb zircon geochronology of granites from the Central Zone, Limopop belt, southern Africa: implications for the age of the Limpopo orogeny. South African Journal of Geology 101, 329–338.

McCourt, S., Hilliard, P., Armstrong, R.A., Munyanyiwa, H., 2001. SHRIMP U–Pb zircon geochronology of the Urungwe Granite, northwest Zimbabwe: age constraints on the timing of the Magondi Orogeny and implications for the correlation between Kheis and Magondi belts. South African Journal of Geology 104, 39–46.

McCourt, S., Vearncombe, J.R., 1992. Shear zones of the Limpopo belt and adjacent granitoid-greenstone terranes: implications for late Archaean collision tectonics in southern Africa. Precambrian Research 9, 127–137.

Modie, B.N.J., 1996. Depositional environments of the meso- to neoproterozoic Ghanzi-Chobe belt, northwest Botswana. Journal of African Earth Sciences 22, 255–268.

Moore, M., Davis, D.W., Robb, L.J., Jackson, M.C., Grobler, D.F., 1993. Archaean rapakivi granite–anorthosite–rhyolite complex in the Witwatersrand basin hinterland, southern Africa. Geology 21, 1031–1034.

Munyanyiwa, H., Krōner, A., Jaeckel, P., 1995. U–Pb and Pb–Pb single zircon ages for charno-enderbites from Magondi mobile belt, northwest Zimbabwe. South African Journal of Geology 98, 52–57.

Rainaud, C., Master, S., Armstrong, R.A., Robb, L.J., 2005. Geochronology and nature of the paleoproterozoic basement in the Central African Copperbelt (Zambia and the Democratic Republic of Congo), with regional implications. Journal of African Earth Sciences 42, 1–31.

Ramokate, L.V., 1998. The geology of Ghanzi-Makunda TLGP project. Bulletin of the Geological Survey of Botswana 43, 54.

Ramokate, L.V., Mapeo, R.B.M., Corfu, F., Kampunzu, A.B., 2000. Proterozoic geology and regional correlation of the Ghanzi-Makunda area, western Botswana. Journal of African Earth Sciences 30, 453–466.

Reeves, C.V., 1978. Reconnaissance aeromagnetic survey of Botswana, 1975–1977. Final interpretation report. Terra Surveys Ltd., Botswana Geological Survey.

Reid, D.L., 1997. Sm–Nd age and REE geochemistry of the Proterozoic arc-related igneous rocks in the Richtersveld subprovince, Namaqua mobile belt, southern Africa. Journal of African Earth Sciences 24, 621–633.

Rollinson, H., Blenkinsop, T., 1995. The magmatic, metamorphic and tectonic evolution of the northern marginal zone of the Limpopo Mobile Belt in Zimbabwe. Journal of the Geological Society of London 152, 65–76.

Schwartz, M.O., Kwok, Y.Y., Davis, D.W., Akanyang, P., 1996. Geology, geochronology and regional correlation of the Ghanzi Ridge, Botswana. South African Journal of Geology 99, 245–250.

Schweitzer, J.K., Hatton, C.J., de Waal, S.A., 1995. Economic potential of the Rooiberg Group: volcanic rocks in the floor and roof of the Bushveld Complex. Minerallium Deposita 3, 168–177.

Singletary, S.J., Hanson, R.E., Martin, M., Bowring, S.A., Key, R.M., Ramokate, L.V., Direng, B.B., Krol, M.A., 2003. Geochronology of basement rocks in the Kalahari Desert, Botswana, and implications for regional tectonics. Precambrian Research 121, 47–71.

Stowe, C.M., 1986. Synthesis and interpretation of structures along the northeastern boundary of the Namaqua Tectonic Province, South Africa. Transactions of the Geological Society of South Africa 89, 185–198.

Stowe, C.W., Hartnady, C.J.H., Joubert, P., 1984. Proterozoic tectonic provinces of southern Africa. Precambrian Research 25, 229–231.

Walraven, F., 1985. Genetic aspects of the granophyric rocks of the Bushveld Complex. Economic Geology 80, 1166–1180.

Walraven, F., 1997. Geochronology of the Rooiberg Group, Transvaal Supergroup, South Africa. University of the Witwatersrand, Economic Geology Research Unit, Information Circular 316.

Walraven, F., Hattingh, E., 1993. Geochronology of the Nebo Granite, Bushveld complex. South African Journal of Geology 96, 31–41.